BRIEF REPORTS

Brief Reports are accounts of completed research which do not warrant regular articles or the priority handling given to Rapid Communications; however, the same standards of scientific quality apply. (Addenda are included in Brief Reports.) A Brief Report may be no longer than four printed pages and must be accompanied by an abstract. The same publication schedule as for regular articles is followed, and page proofs are sent to authors.

Construction of invariant tori in chaotic regions

Mikko Kaasalainen
NORDITA, Blegdamsvej 17, 2100 Copenhagen, Denmark
(Received 2 December 1994; revised manuscript received 24 February 1995)

Following the introduction of a general method for constructing approximate invariant tori of a given Hamiltonian H [M. Kaasalainen and J. J. Binney, Phys. Rev. Lett. **73**, 2377 (1994)], it is shown that the scheme can be applied to Hamiltonians with globally chaotic regions as well. The created tori are proper in that (i) they are geometrically credible and fill chaotic regions in an orderly way; (ii) their frequencies are consistent with those of the closed orbits of H; and (iii) for short time periods, motion on them approximates motion in H. One of the examples is given in a rotating frame of reference, with a Hamiltonian more complicated than the usual sum of kinetic and potential energies.

PACS number(s): 05.45.+b, 03.20.+i, 95.10.Fh, 98.10.+z

The computation of the invariant phase-space tori of Hamiltonian systems is an important problem in several fields (see Ref. [1] and references therein). Recently [1–4], techniques have been developed for nonperturbatively determining a canonical transformation that maps the invariant tori of an integrable "toy" Hamiltonian H_T into approximately invariant tori of a given "target" Hamiltonian H; the transformation between the ordinary phase-space coordinates $\mathbf{w} \equiv (\mathbf{p}, \mathbf{x})$ and the action-angle coordinates $(\mathbf{J}, \boldsymbol{\theta})$ of H_T is known. With the methods of Refs. [1–3], it is possible to construct invariant tori of a given type also in regions of phase space where there are no invariant tori of H of that type. Such regions are filled in an orderly way by the constructed tori; these can be seen as invariant tori of an integrable Hamiltonian H_0 that closely approximates H, and shares with H whatever invariant tori H may possess [1,5].

The examples of Refs. [1–6] concern regions of regular or locally stochastic motion; the latter is seen in a Poincaré surface of section as the stochastic layer around a separatrix bounding an island. In globally chaotic regions, stochasticity is no longer contained in such layers. It is desirable for the construction methods to be applicable also to Hamiltonians H producing such regions. One can view such an H as a large perturbation of an integrable H_0: as the perturbation is increased, fewer and fewer invariant (KAM) tori survive, and finally they all disappear. Thus, in determining an H_0 by interpolation between the constructed tori [1,5], one cannot usually employ KAM-tori of H alone, but necessarily has to construct tori of H_0 directly in the chaotic regions.

In the following, tori are constructed with the generating function approach described in Ref. [1]; the toy Hamiltonian H_T is the two-dimensional harmonic oscillator, because its orbits are topologically similar to the so-called "box" orbits that are of interest here. Tori are described by the action-angle variables and the frequencies $\boldsymbol{\omega}$; we employ the convention that unprimed $\mathbf{J}, \boldsymbol{\theta}, \boldsymbol{\omega}$ relate to the tori of H_T, while the primed ones correspond to those of H_0. We seek a generating function $S(\boldsymbol{\theta}, \mathbf{J}')$ of the form

$$S(\boldsymbol{\theta}, \mathbf{J}') = \boldsymbol{\theta} \cdot \mathbf{J}' - i \sum_{\mathbf{n} \neq 0} S_{\mathbf{n}}(\mathbf{J}') \exp(i\mathbf{n} \cdot \boldsymbol{\theta}), \tag{1}$$

that maps the tori of H_T into those of H_0. The toy and target actions and angles are related by

$$\mathbf{J} = \partial S(\boldsymbol{\theta}, \mathbf{J}')/\partial \boldsymbol{\theta}, \ \boldsymbol{\theta}' = \partial S(\boldsymbol{\theta}, \mathbf{J}')/\partial \mathbf{J}'. \tag{2}$$

The Levenberg-Marquardt (nonlinear least-squares optimization) algorithm is used to find the coefficients $S_{\mathbf{n}}$ that minimize the variation of H over the trial torus of given $\mathbf{J}'$.

As in Ref. [1], the examples here concern motion in the logarithmic potential

$$\Phi(x, y) = \frac{1}{2} \ln \left(x^2 + \frac{y^2}{q^2} + R_c^2 \right), \tag{3}$$

where $R_c = 0.14$ and q is varied in the range $(0, 1]$. This represents a nonaxisymmetric planar gravitational potential, such as that of an elongated galaxy [7].

Motion in the unadorned potential (3) is known to be very regular: when the parameter q is made smaller, more and more resonant islands appear, but stochasticity is always contained in local layers, never spreading to larger

regions of phase space. One way of creating increased stochasticity is to add an irregularity term to (3), as in Ref. [7]:

$$\Phi_{\rm irr} = \frac{1}{2}\ln\left[x^2 + \frac{y^2}{q^2} + R_c^2 - \left(\frac{r}{s}\right)(x^2 - y^2)\right], \qquad (4)$$

where $r \equiv \sqrt{x^2+y^2}$, and s is an additional parameter. It should be noted that, by rescaling x and y, the potential (4) can be rewritten as one governed by one parameter appearing in a constant term as R_c in (3), without using two parameters s and R_c. The parameter s is used here merely to show how large the contribution of the irregularity term is, as compared to (3), when R_c is kept fixed.

Let us perturb the regular motion presented in Fig. 1 of Ref. [1] by setting $s = 3.5$ at $q = 0.8$ and $H = -0.199$, and construct tori for the major family of "box" orbits. The corresponding $(x, \dot{x})$ section is shown in Fig. 1. Box orbits are now globally chaotic except for the islands of stability associated with the resonances 1:2 (the outermost island), 2:3, and some others. Nevertheless, the constructed tori retain the same form as in the regular case. The least-squares method is thus able to construct good tori even in a wide chaotic region. Moreover, the ratios ω_1'/ω_2' of the frequencies assigned to the uppermost two tori bound 2/3 on both sides: one can treat the islands of the minor-orbit family as caused by a perturbed 2:3 resonance of a constructed H_0, as in Ref. [1]. The lower pair bounds a 3:4 resonance: the corresponding islands have practically drowned in the stochastic sea, but the curves still "remember" how the islands were located in the case of a smaller irregularity term. The method of determining the frequencies $\boldsymbol{\omega}'$ and angle coordinates $\boldsymbol{\theta}'$ for a single constructed torus incorporates the principle of linear time development of the angles along a trajectory on an invariant torus [1]:

$$\boldsymbol{\theta}' = \boldsymbol{\theta}_0' + \boldsymbol{\omega}' t. \qquad (5)$$

If the created torus approximates an existing invariant torus of H, the motion (5) on the torus will approximate the time development of a phase space trajectory $\mathbf{w}(t)$ given by H. If the torus is constructed in a resonant or stochastic region of H, one is free to define how (5) projects into $\mathbf{w}(t)$: the method of Ref. [1] assigns credible frequencies and angles to such a torus.

Another very interesting way of creating global stochasticity is to set (3) to rotate with an angular velocity $\boldsymbol{\Omega} = \Omega\hat{\mathbf{z}}$, where $\hat{\mathbf{z}}$ is the z-axis unit vector, and study the Hamiltonian in the rotating frame of reference. Astrophysically this is of interest, because from observations it is known that the potential figures of galaxies typically rotate.

First, let us write the Hamiltonian in a rotating frame of reference. This can be done by using a time-dependent canonical transformation between the inertial and the rotating frame. The canonical variables in the rotating frame are denoted by $(\mathbf{p}, \mathbf{x})$ and those in the inertial frame by $(\mathbf{p}', \mathbf{x}')$. Now

$$\mathbf{x}'(\mathbf{x}, t) = \mathbf{x}\cos\Omega t + \hat{\mathbf{z}} \times \mathbf{x}\sin\Omega t. \qquad (6)$$

[In the three-dimensional case, (6) holds for x and y coordinates; z and p_z are, of course, invariant.] This transformation can be generated by the function $F(\mathbf{p}', \mathbf{x}, t) = \mathbf{p}' \cdot \mathbf{x}'(\mathbf{x}, t)$; from $\partial F/\partial \mathbf{p}'$ we have (6), and $\mathbf{p} = \partial F/\partial \mathbf{x}$. The Hamiltonian H in the rotating frame follows from the inertial Hamiltonian H' by

$$H = H' - \frac{\partial F}{\partial t} = \frac{1}{2}p^2 + \boldsymbol{\Omega} \cdot (\mathbf{p} \times \mathbf{x}) + \Phi(\mathbf{x}). \qquad (7)$$

The cross (Coriolis) term makes this Hamiltonian asymmetric under time reversal. Also, the canonically conjugate momenta $\mathbf{p}$ are no longer just the Cartesian coordinate velocities as in the inertial space; from the Hamiltonian equations of motion we have

$$\dot{\mathbf{x}} = \frac{\partial H}{\partial \mathbf{p}} = \mathbf{p} - \boldsymbol{\Omega} \times \mathbf{x}. \qquad (8)$$

The Newtonian equations of motion can be obtained by taking the time derivative of (8) and combining that with

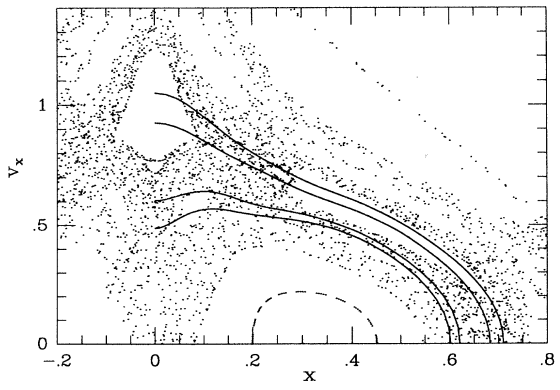

FIG. 1. $(x, \dot{x})$ section for the modified logarithmic potential (4) with $q = 0.8$ and $s = 3.5$ at $H = -0.199$. Dots are integrated consequents, and the solid lines are curves of numerically constructed tori. For clarity, the islands of stability have been left empty.

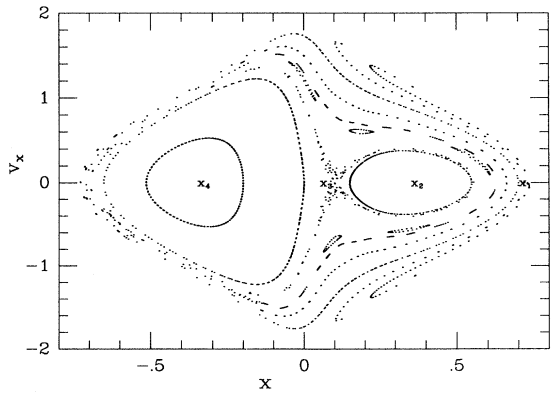

FIG. 2. $(x, \dot{x})$ for the Hamiltonian (7) at $H = -0.315$ with $q = 0.9$ and $\Omega = 0.3$. The orbit families x_1–x_4 (x_3 at an unstable point) are marked.

$\dot{\mathbf{p}} = -\partial H/\partial \mathbf{x}$:

$$\ddot{\mathbf{x}} = -\frac{\partial \Phi_{\text{eff}}}{\partial \mathbf{x}} - 2(\boldsymbol{\Omega} \times \dot{\mathbf{x}}), \tag{9}$$

where the effective potential Φ_{eff} is

$$\Phi_{\text{eff}} = \Phi - \frac{1}{2}\Omega^2(x^2 + y^2). \tag{10}$$

The value of the Hamiltonian (7) is called the Jacobi constant E_J, which can also be written in terms of the Cartesian noncanonical variables as $E_J = \frac{1}{2}|\dot{\mathbf{x}}|^2 + \Phi_{\text{eff}}$.

As is well known [7], rotating barred potentials produce four kinds of major families: loop orbits around stable closed ones, usually labelled x_1, x_2, and x_4 (x_3 corresponds to an unstable orbit), plus the box orbits. Figure 2 shows the $(x, \dot{x})$ section of the logarithmic potential with $q = 0.9$ at $H = -0.315$ and rotation speed $\Omega = 0.3$. (At $y = 0$, the momentum p_1 coincides with $\dot{x}$.) The loop orbit families are quite regular and not very interesting in this context, whereas among the boxes one will find large regions of stochasticity as the rotation speed is increased. As previously, the boxes can be handled with the harmonic oscillator as the toy Hamiltonian. Previously, the target action values for the sets of major-type tori could be arranged to join smoothly in a natural way in the action space; now, the corresponding action patches overlap and leave gaps [8]. Thus, if one creates an integrable Hamiltonian from the constructed tori, it applies to each major family separately.

In the time-symmetric case, the imaginary parts of the Fourier coefficients of the generating function S, as given in (1), vanish; geometric symmetries affect some more coefficients [2,3]. In the time-asymmetric case, the structure of the Fourier series can be deduced, e.g., from the general shapes of the invariant curves in surfaces of section. For the box orbits in the present case, one finds that (denoting the real and imaginary parts of the coefficients $S_{\mathbf{n}}$ by superscripts R and I) S contains only terms $S^R_{\mathbf{n}}$ with both indices of $\mathbf{n}$ even (as in the nonrotating case), and terms $S^I_{\mathbf{n}}$ with both indices of $\mathbf{n}$ odd.

In Fig. 3 the $(x, \dot{x})$ section at $H = -0.253$, $q = 0.8$, and $\Omega = 0.4$ is shown. The x_2 family has now vanished. The solid lines are the invariant curves of constructed box-type tori. In this case, the box orbits are almost rectangular in configuration space, so an additional point transformation [1] is not used. In the Fourier series for S, the coefficients $S^R_{\mathbf{n}}$ and $S^I_{\mathbf{n}}$ decrease in $\mathbf{n}$ in a regular manner — the number of coefficients is about two times that needed for time-symmetric Hamiltonians. The need for many $S^I_{\mathbf{n}}$ is obvious from the asymmetry of the surface of section with respect to the momentum axis.

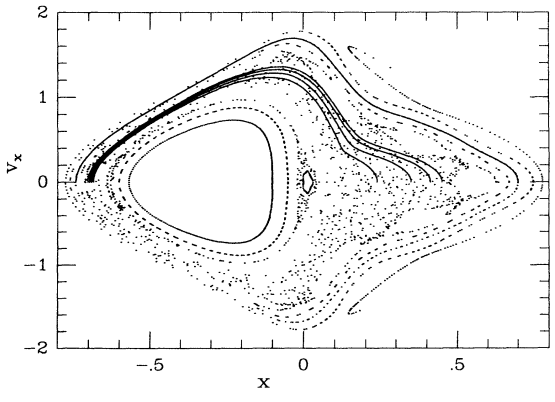

FIG. 3. $(x, \dot{x})$ at $H = -0.253$ with $q = 0.8$ and $\Omega = 0.4$. The solid curves are those of constructed tori.

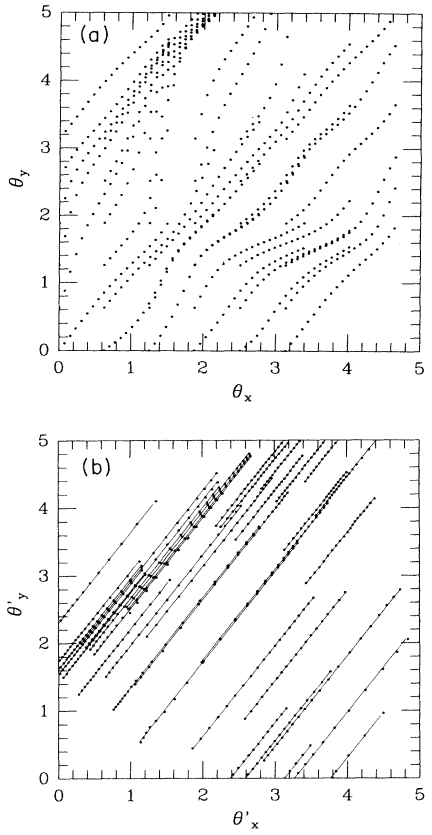

FIG. 4. (a) Trajectories in toy angle $\boldsymbol{\theta}$ space obtained by direct integration of the equations of motion from several starting points on the middle torus of Fig. 3. (b) The same trajectories in target angle $\boldsymbol{\theta}'$ space (dots), together with the semianalytical linear trajectories (5) (straight lines).

The tori constructed in the chaotic region are again perfectly credible. Note how the curves of the constructed tori mimic well the behavior of the invariant curves that "used to" lie in the now chaotic region before the fast rotation dissolved them (cf. Fig. 2). The assigning of the target angles and frequencies is illustrated in Fig. 4 (compare with Fig. 3 of Ref. [1]). Note that even though the motion on the integrated strips certainly does not occur on a torus, and cannot thus coincide with a linear increase in the created target angles, the linear strips in Fig. 4(b), corresponding to the middle torus of Fig. 3, are still very close to target angle points corresponding to the integrated strips. Thus, for short time periods, motion on the constructed torus approximates motion in H as well as possible because of (i) the way the torus

is fitted in phase space, and (ii) the way the angles and frequencies are determined.

An interesting thing about the chaotic region is that it stops very sharply at the outer edge of the large 5:7 islands seen in Fig. 3. A series of invariant curves starts immediately after the islands, going then over to the separate region of the x_1 family. Eventually, the insides of boxes break up because of the Coriolis effect, and the loop-type x_1 orbits are formed. These cannot be mapped as boxes with the harmonic oscillator any more, because they leave a gap around the origin in configuration space. Accordingly, the boundary of a box orbit close to the x_1 family is roughly rectangular all right, but motion inside it is different from that of the harmonic oscillator. Consequently, the Fourier series for the generating function S becomes quite long. In this case, the tori produced by the least-squares method (with computationally reasonable resolution and number of coefficients) do not coincide accurately with the invariant curves between the 5:7-islands and the x_1 family. However, the orbit integration method can be employed to improve the accuracy [4,1]. Now one can obtain a perfect fit to the integrated consequents, as can be seen from the outermost solid curve in Fig. 3.

The above example illustrates the useful complementary nature of the two torus-construction techniques. The orbit integration method is very useful for obtaining accurate approximations to the existing invariant tori of H, especially in difficult cases when the number of significant coefficients in the series for S is large. In the above case, one could also have used the harmonic oscillator in a rotating frame of reference as the toy Hamiltonian H_T for the difficult boxes (for its actions and angles see Ref. [9]); however, the methods at our disposal work well with the ordinary harmonic oscillator as well.

The examples in this paper demonstrate the general applicability of the torus-construction scheme of Ref. [1]: "artificial" tori can be created even for Hamiltonians that possess very few invariant tori of their own. Especially when constructing an integrable Hamiltonian H_0 close to a given nonintegrable one, H, it is possible to create tori on a grid in action space without having to worry about stochastic regions. Having such an H_0 at one's disposal should make it possible to, for example, apply perturbation theory in studying the onset of chaos and phenomena occurring near and between resonances.

[1] M. Kaasalainen and J.J. Binney, Phys. Rev. Lett. **73**, 2377 (1994).
[2] C. McGill and J.J. Binney, Mon. Not. Roy. Astron. Soc. **244**, 634 (1990).
[3] M. Kaasalainen and J.J. Binney, Mon. Not. Roy. Astron. Soc. **268**, 1033 (1994).
[4] R. Warnock, Phys. Rev. Lett. **66**, 1803 (1991).
[5] R. Warnock and R. Ruth, Phys. Rev. Lett. **66**, 990 (1991); Physica D **56**, 188 (1992).
[6] M. Kaasalainen, Mon. Not. Roy. Astron. Soc. **268**, 1041 (1994).
[7] J.J. Binney and S. Tremaine, *Galactic Dynamics* (Princeton University Press, Princeton, 1987).
[8] J.J. Binney and D. Spergel, Mon. Not. Roy. Astron. Soc. **206**, 159 (1984).
[9] K. Freeman, Mon. Not. Roy. Astron. Soc. **133**, 47 (1966).